

# Generation of attenuation compensating Airy beams

Miguel A. Preciado,<sup>1,\*</sup> Kishan Dholakia,<sup>1</sup> and Michael Mazilu<sup>1</sup>

<sup>1</sup>*SUPA, School of Physics and Astronomy, University of St. Andrews, North Haugh, St. Andrews, KY16 9SS, UK.*

*\*Corresponding author: ma.preciado@upm.es*

Compiled July 18, 2014

We present an attenuation corrected “non-diffracting” Airy beam. The correction factor can be adjusted to deliver a beam that exhibits an adjustable exponential intensity increase or decrease over a finite distance. A digital micro-mirror device (DMD) that shapes both amplitude and phase is used to experimentally verify the propagation of these beams through air and partially absorbing media. © 2014 Optical Society of America  
*OCIS codes:* (140.3300), (260.1960), (070.2580), (070.3185), (070.7345)

Propagation-invariant light fields have attracted significant attention due to their ability to retain their transverse profile during propagation over finite distances. The family of such beams includes Bessel, Matthieu and the Airy light modes. The Airy wavepackets were first proposed in 1979 [1], within the context of quantum mechanics, and experimentally realised in the optical domain in 2007 [2]. These light fields exhibit self-healing properties [3], have been used for spatio-temporal light-bullets under linear and non-linear conditions [4–6], in the field of plasmonics [7] and optical micromanipulation [3]. More recently, the Airy fields have found applications for super-resolved and light-sheet microscopy [8,9]. Most of these applications are motivated by the self-healing, non-linear and “non-diffractive” propagation nature of the Airy beam. However, these properties are only maintained in isotropic lossless media. Propagation through absorbing media leads to an exponentially intensity decay in the propagation direction of the beam. Here, we show that it is possible to counteract this behaviour by modifying the Airy beam to compensate, over a finite distance, for this effect. A similar compensation was proposed and numerically demonstrated [10] in the temporal domain and we use this as our starting point. By applying the duality between the equations that describe the paraxial diffraction of spatially confined light beams and the dispersion of narrow-band pulses in dielectrics (so called, space-time duality) [11], an equivalent compensating Airy beam is proposed in this letter for spatial optics, and experimentally demonstrated. Furthermore, we generate the field with a digital micromirror device (DMD), used in this instance for complex field (amplitude/phase) spatial light modulation. A DMD chip is composed by an array of microscopic mirrors that can be individually rotated into two positions, each of them leading to an on/off modulation of the reflected output beam at that specific pixel position. This results in a binary amplitude modulation of the incident light beam according to the micro-mirror state. DMDs show a number of advantages such as speed, precision, polarization insensitivity, broadband capability and damage thresholds when

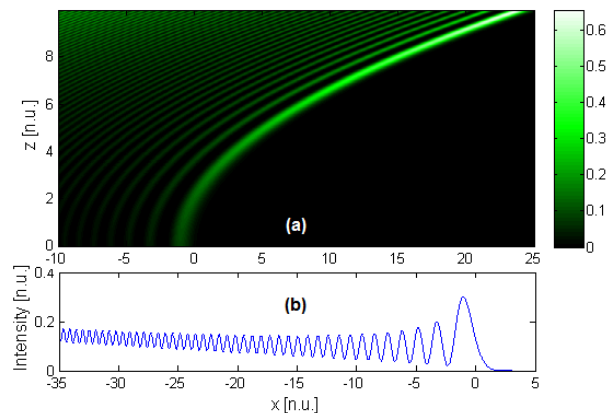


Fig. 1. (color online) Intensity profile of the attenuation compensating Airy beam as it propagates through a losses medium with  $x_0 = 1$ ,  $z_0 = 1$ ,  $\alpha = 0$  and  $b_0 = 0.2$ . (a)  $x$ - $z$  intensity density plot (b) Cross section in the apex plane  $z = 0$ .

compared with liquid crystal spatial light modulator. Their modulation efficiency depends on several technological parameters (pixel fill factor, diffraction efficiency, micromirrors reflectance,...) [12], and is ultimately limited by the binary amplitude holograms optimum efficiency of 10% [13]. DMD technology has already been successfully proven as an efficient alternative for spatial light modulation for beam shaping such as the generation of Laguerre-Gaussian [14–16] and of propagation invariant fields [17,18]. This method of generating beams enables the reconfiguration of beams at a very fast rate (kHz) [15]. We use this emergent technology for creating the proposed attenuation compensating Airy beams.

We begin by describing the theoretical basis of the proposed attenuation compensating Airy beam and its propagation properties. The one dimensional Airy beam field, in the apex plane, is defined by  $u_0(x) = \text{Ai}(x/x_0)$  where  $x$  is the transversal coordinate and  $x_0$  its scaling factor. Its associated Fourier transform, in the reciprocal space defined by  $k_x$ ,

$$\hat{u}_0(k_x) = x_0 \exp(ix_0^3 k_x^3/3), \quad (1)$$

shows the characteristic cubic phase profile and defines the spatial spectrum of the Airy beam. The attenuation compensating Airy beam is created through a variable amplification factor of each spectral component defined by  $\exp(-b_0 k_x)$ . Using the Huygens-Fresnel integral in the reciprocal space, we can determine the beam spatial spectrum after propagating a distance  $z$  through a linearly absorbing media:

$$\hat{u}(k_x, z) = \exp\left(\frac{ik_x^2 z}{2k} - ikz\right) \hat{u}_0(k_x) \exp(-b_0 k_x) \quad (2)$$

where  $k = n_0 k_0 - i\alpha/2$  is the complex wave-vector defined to include the vacuum wave-vector  $k_0 = 2\pi/\lambda$  and index of refraction  $n_0$  and absorption coefficient  $\alpha$  of the medium. Considering a bandwidth limited Airy beam  $|k_x| \leq k_{max}$  and distances of propagation  $z \ll 4n_0^2 k_0^2 / (\alpha k_{max}^2)$  we can approximate the propagation evolution to:

$$\hat{u}(k_x, z) \approx \exp\left(\frac{ik_x^2 z}{2n_0 k_0} - ikz\right) \hat{u}_0(k_x) \exp(-b_0 k_x). \quad (3)$$

By performing an inverse Fourier transform of this spatial spectrum, we can determine the beam field associated with the compensated beam at any propagation position  $z$ :

$$u(x, z) = \text{Ai}\left(\frac{x}{x_0} - \frac{z^2}{4z_0^2} + \frac{ib_0}{x_0}\right) \exp\left(-\frac{\alpha z}{2} + \frac{zb_0}{2z_0 x_0}\right) \exp\left(\frac{iz^3}{12z_0^3} - \frac{iz_0 z}{x_0^2} - \frac{izx}{2z_0 x_0}\right) \quad (4)$$

where  $z_0 = n_0 k_0 x_0^2$  is associated to the opening parameter of the parabolic trajectory of the Airy beam. It is the  $zb_0/(2z_0 x_0)$  term that counteracts the exponential field decay in a linearly absorbing medium. Indeed, the overall compensated intensity loss is given by  $\alpha - b_0/(z_0 x_0)$ . Figure 1 shows the cross section of this beam and its propagation behaviour through a non absorbing medium. In short, we can understand this beam by considering an exponential amplification in reciprocal space. This amplification counteracts the intensity loss due to linear absorption when viewing the Airy beam as the superposition of multiple plane waves forming a caustic corresponding to the main lobe of the Airy beam. The exponential amplification increases in effect the amplitude of the constituent plane waves such that taking into account the absorption, these plane waves "reach" the main lobe having the same amplitude. The two dimensional Airy beam can be treated in a similar way and corresponds to the product between two complex fields  $u(z, x)u(z, y) \exp(ikz)$  where the last term cancels out the double counted carrier wave. In this case, the attenuation compensated Airy beam has a compensated loss term defined  $\gamma = \alpha - (b_{0x} + b_{0y})/(z_0 x_0)$  where  $b_{0x}$  and  $b_{0y}$  correspond to the compensation factors for the  $u(z, x)$  and  $u(y, z)$  fields. We also note that the attenuation compensation behaviour is also present for finite energy Airy beams.

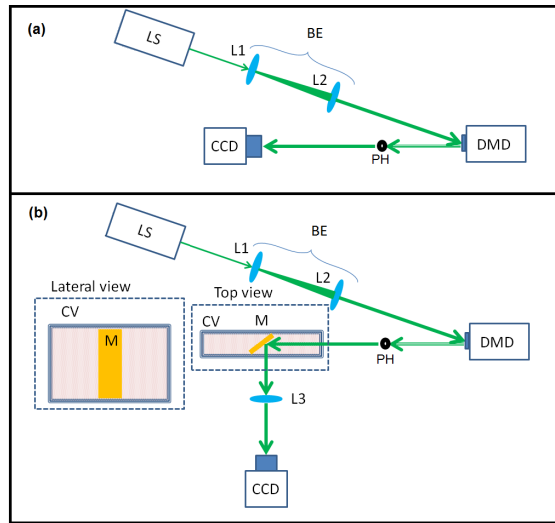


Fig. 2. (color online) Set up for lossless (air) (a) and lossy (Rhodamine-B solution) (b) Airy beam propagation experiments. LS: Laser source; BE: Beam Expander; M: Mirror; CV: Cuvette with solution; L1, L2, L3: Lenses; CCD: Charge coupled device camera; DMD: Digital Micromirror Device; PH: Pinhole.

In order to demonstrate the “diffraction-free” propagation and simultaneous attenuation compensation of the proposed finite energy Airy-based beam, we designed, numerically simulate, and experimentally demonstrate three attenuation compensated Airy beam examples. The laser source used is a Helium-Neon laser ( $\lambda = 543$  nm) chosen to optimise the diffraction efficiency of the DMD. We considered two propagation media: one lossless reference media corresponding to propagation through air and one lossy propagation media consisting of a Rhodamine-B solution in water, with a measured absorption, due to fluorescence, of  $\alpha = 2.97$  dB/cm. The beams are generated using a commercial DMD (Texas Instruments DLP Lightcrafter EVM), which provides a cost-effective, easily reproducible solution for spatial light modulation, with the possibility of dynamically changing the modulation at a kHz rate. After a careful design underpinned by numerical simulations, aimed to show a significant attenuation compensation of our experiment dimensions, we have selected the parameters  $x_0 = 2.78 \times 10^{-5}$  m and  $b_{0x} = b_{0y} = q \cdot 1.84 \times 10^{-6}$  m, where  $q = 0, 1, \text{ and } 2$ , respectively for first, second and third beam example (note that the first example corresponds to a “classic” Airy beam). These values lead to an overall intensity loss factors  $\gamma = 2.97 - q \cdot 0.97$  dB/cm in the Rhodamine-B solution in water (with  $n_0 = 1.33$ ). In air (with  $n_0 = 1$ , and  $\alpha = 0$ ) we obtain  $\gamma = -q \cdot 1.29$  dB/cm. A finite energy beam is obtained by windowing in spectral domain, applying an 8th-order super-Gaussian flat-top window,  $W(k_x, k_y) = \exp(-k_x^8 / (2k_{max}^8)) \exp(-k_y^8 / (2k_{max}^8))$ , where  $k_{max} = 1.77 \times 10^4$  m $^{-1}$ . We design the desired beam functions to be focused at a central position 12 cm after

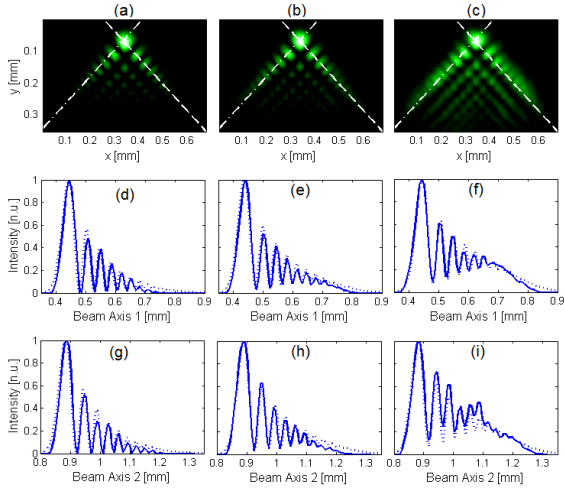


Fig. 3. Beam intensity function captured with the CCD after 11 cm of lossless propagation (a,b, and c) for first, second and third examples, where beam axes '1' and '2' are showed in white dotted and dash-dotted line, respectively; measured (solid) and numerically simulated (dashed) beam intensity across beam axes '1' (d, e and f) and '2' (g, h, and i) for first, second and third beam example, respectively.

the DMD surface by pre-compensating the diffraction corresponding to 12 cm of free-space propagation.

By using an approximately uniform illumination on the DMD modulation area, we can consider the desired spatial modulation functions to be approximately equal to the previously designed beam complex field functions. Moreover, it is possible to codify a complex (amplitude/phase) spatial modulation  $\psi(x, y) \in \mathbb{C}$  in the binary amplitude spatial modulation delivered by the DMD [14, 16]. Here, we consider a two step encoding procedure. In a first step, we create a real non-negative diffraction mask  $f(x, y)$  associated with the complex modulation  $\psi(x, y)$  by using

$$f(x, y) = f_0(x, y) + f_{+1}(x, y) + f_{-1}(x, y) = |\psi(x, y)| + \text{Re} \left( \psi(x, y) e^{i(k_x x + k_y y)} \right) \quad (5)$$

where the diffraction mask leads to three diffraction orders  $f_0(x, y) = |\psi(x, y)|$ ,  $f_{+1}(x, y) = \frac{1}{2} \psi(x, y) e^{i(k_x x + k_y y)}$ ,  $f_{-1}(x, y) = \frac{1}{2} \psi^*(x, y) e^{i(-k_x x - k_y y)}$ , each of them generating a modulated beam in an angle defined by the mask wavevector  $(k_x, k_y)$ . A pinhole selection of the diffraction order  $f_{+1}(x, y)$  provide our desired complex modulation  $\psi(x, y)$ . Finally, the real non-negative modulating function  $f(x, y)$  can be quantized by applying a binary dithering algorithm, resulting in a binary amplitude modulating function. More specifically, a Floyd-Steinberg error-diffusion dithering algorithm is used here [19], where the resulting binary distribution is calculated by diffusing the residual quantization error of a quantized pixels onto their neighboring pixels.

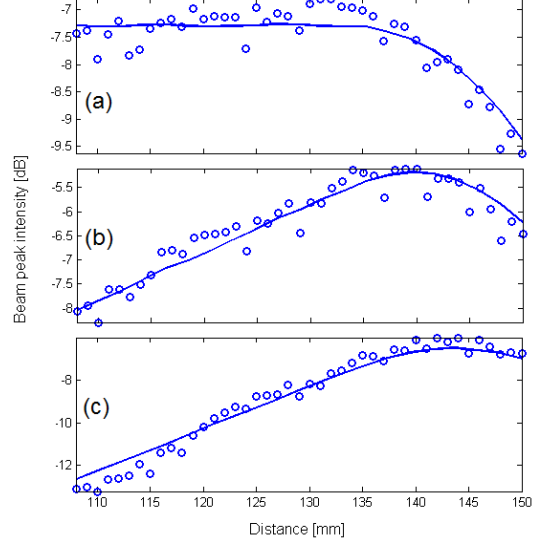


Fig. 4. Beam peak intensity during the lossless propagation from numerical simulation (solid) and experimental measurements (circle-dashed) for first (a), second (b), and third (c) beam example, designed to exhibit an exponential growth of 0, 1.29 and 2.48 dB/cm, respectively.

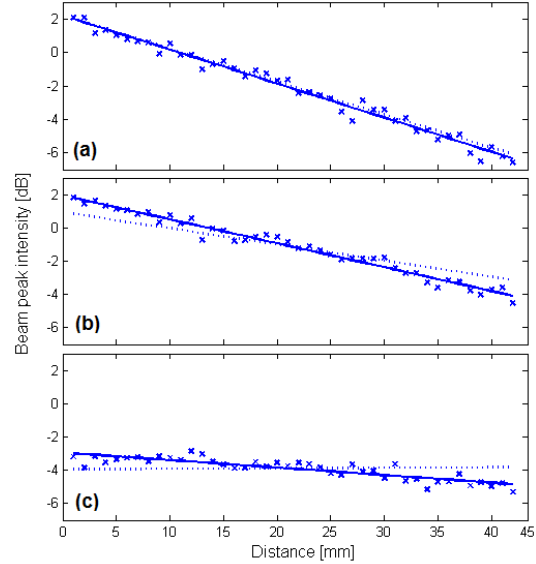


Fig. 5. Peak intensity along a path of lossy medium propagation inside the cuvette containing the Rodhamine-b water solution, obtained from experimental measurements (crosses), and linear fit (solid), compared to the theoretically expected peak intensity evolution (dashed) for first (a), second (b), and third (c) beam example, respectively.

In order to verify the correct modulation of the beams, we use the set up depicted in Fig. 2(a) for free-space propagation. An expanded and collimated beam from the laser source is modulated by the DMD with the previously calculated binary spatial modulating functions. Figure 3 shows the resulting beam captured by the CCD at 11 cm from the DMD modulating surface, where the beam profile across the Airy beam axes is represented, and compared to those predicted by numerical simulations. The resulting propagating beams are captured by a CCD camera at different distances. The beam peak intensity as a function of the distance to the DMD modulation plane is represented in Fig. 4 and compared to the numerically simulated beam peak intensity. In these examples, we obtain the theoretically predicted positive linear logarithmic (i.e. increasing exponentially) evolution of the beam maximum along the propagation path.

Finally, in order to show the attenuation compensation property of the resulting beams, we use the set-up shown in Fig. 2(b), where a cuvette 5 cm long (in propagation direction  $z$ ), 1 cm width and 12.5 cm height is filled with the solution of Rhodamine-B in water. In order to measure the beam peak intensity inside the cuvette, we fabricated a customized size square gold mirror, designed to fit inside the cuvette as showed in Fig. 2(b), which was made by deposition of a gold layer on a glass surface. The reflected beam is captured by a CCD camera focused at the reflection point. Figure 5 shows the measured beam intensity peak of the three beams considered. We observe that the third beam compensates best for the Rhodamine-B absorption. Interesting to note that the output peak intensity in Fig. 5a is smaller than the one observed in Figures 5b,c. Considering a perfect beam shaping filter, it is impossible to achieve a larger output peak intensity as the attenuation correction mask discussed here has no gain. However, due to the DMD encoding, an apparent amplification resulting from higher diffraction efficiency might be observed for specific masks.

In conclusion, we have proposed a novel form of Airy function based beams exhibiting attenuation compensating propagation. We have experimentally demonstrated that this unique propagation property remains in the finite-energy beam after the spectral truncation of the ideal infinite-energy beams. The proposed Airy beams may find interest in accelerating beam based applications such as imaging [8], plasmonics [7] and micro manipulation, particularly where the attenuation compensating propagation can be used to obtain a more uniform peak intensity across the propagation path of lossy or highly scattering media. It is worth noting that it might be possible to obtain other more generic peak intensity modulation profiles in a similar way as proposed here. This would broaden the range of possible applications of the intensity engineered Airy beam. We have additionally shown the possibility of using a DMD for such beam generation, which offers a cost-effective solution, and the possibility of working with spatial modulation

at kHz rates suitable for imaging and other applications.

## References

1. M. Berry and N. Balazs, *Am. J. Phys* **47**, 264–267 (1979).
2. G. A. Siviloglou, J. Broky, A. Dogariu, and D. N. Christodoulides, *Phys. Rev. Lett.* **99**, 213901 (2007).
3. J. Baumgartl, M. Mazilu, and K. Dholakia, *Nature Photonics* **2**, 675–678 (2008).
4. A. Chong, W. H. Renninger, D. N. Christodoulides, and F. W. Wise, *Nature Photonics* **4**, 103–106 (2010).
5. D. Abdollahpour, S. Suntsov, D. G. Papazoglou, and S. Tzortzakis, *Physical Review Letters* **105**, 253901 (2010).
6. P. Polynkin, M. Kolesik, and J. Moloney, *Physical Review Letters* **103**, 123902 (2009).
7. A. Salandrino and D. N. Christodoulides, *Optics Letters* **35**, 2082–2084 (2010).
8. T. Vettenburg, H. I. C. Dalgarno, J. Nylk, C. Coll-Llado, D. E. K. Ferrier, T. Cizmar, F. J. Gunn-Moore, and K. Dholakia, *Nat Meth* **11**, 541–544 (2014).
9. S. Jia, J. C. Vaughan, and X. Zhuang, *Nat Photonics* **8**, 302–306 (2014).
10. M. A. Preciado and K. Sugden, *Optics Letters* **37**, 4970–4972 (2012).
11. B. Kolner, *Quantum Electronics, IEEE Journal of* **30**, 1951–1963 (1994).
12. H. Ryoo, D. W. Kang, and J. W. Hahn, *Microelectron. Eng.* **88**, 235–239 (2011).
13. B.R. Brown and A.W. Lohmann in *IBM Journal of Research and Development* **13**, 160–168 (1979).
14. Y.-X. Ren, M. Li, K. Huang, J.-G. Wu, H.-F. Gao, Z.-Q. Wang, and Y.-M. Li, *Applied optics* **49**, 1838–1844 (2010).
15. M. Mirhosseini, O. S. M. na Loaiza, C. Chen, B. Rodenburg, M. Malik, and R. W. Boyd, *Opt. Express* **21**, 30196–30203 (2013).
16. V. Lerner, D. Shwa, Y. Drori, and N. Katz, *Optics letters* **37**, 4826–4828 (2012).
17. L. Gong, Y.-X. Ren, G.-S. Xue, Q.-C. Wang, J.-H. Zhou, M.-C. Zhong, Z.-Q. Wang, and Y.-M. Li, *Appl. Opt.* **52**, 4566–4575 (2013).
18. Q. Xu, Y. Wang, S. Siew, J. Lin, and Y. Zhang, *Applied Physics B*, doi:10.1007/s00340-014-5813-2 (posted 7 May 2014, online).
19. R. Floyd and L. Steinberg, in *Proc. Soc. Inf. Disp.* **17**, 75–77 (1976).

## Acknowledgments

We thank Andrea Di Falco for the fabrication of the customized size gold mirrors. This research was supported by the UK Engineering and Physical Sciences Council Programme Grant EP/J01771X/1 and Royal Society research grant RG130854.

## References

1. M. Berry and N. Balazs, "Nonspreading wave packets," *Am. J. Phys* **47**, 264–267 (1979).
2. G. A. Siviloglou, J. Broky, A. Dogariu, and D. N. Christodoulides, "Observation of accelerating Airy beams," *Phys. Rev. Lett.* **99**, 213901 (2007).
3. J. Baumgartl, M. Mazilu, and K. Dholakia, "Optically mediated particle clearing using Airy wavepackets," *Nature Photonics* **2**, 675–678 (2008).
4. A. Chong, W. H. Renninger, D. N. Christodoulides, and F. W. Wise, "Airy–bessel wave packets as versatile linear light bullets," *Nature Photonics* **4**, 103–106 (2010).
5. D. Abdollahpour, S. Suntsov, D. G. Papazoglou, and S. Tzortzakis, "Spatiotemporal airy light bullets in the linear and nonlinear regimes," *Physical Review Letters* **105**, 253901 (2010).
6. P. Polynkin, M. Kolesik, and J. Moloney, "Filamentation of femtosecond laser Airy beams in water," *Physical Review Letters* **103**, 123902 (2009).
7. A. Salandrino and D. N. Christodoulides, "Airy plasmon: a nondiffracting surface wave," *Optics Letters* **35**, 2082–2084 (2010).
8. T. Vettenburg, H. I. C. Dalgarno, J. Nylk, C. Collado, D. E. K. Ferrier, T. Cizmar, F. J. Gunn-Moore, and K. Dholakia, "Light-sheet microscopy using an Airy beam," *Nat Meth* **11**, 541–544 (2014).
9. S. Jia, J. C. Vaughan, and X. Zhuang, "Isotropic three-dimensional super-resolution imaging with a self-bending point spread function," *Nat Photonics* **8**, 302–306 (2014).
10. M. A. Preciado and K. Sugden, "Proposal and design of Airy-based rocket pulses for invariant propagation in lossy dispersive media," *Optics Letters* **37**, 4970–4972 (2012).
11. B. Kolner, "Space-time duality and the theory of temporal imaging," *Quantum Electronics, IEEE Journal of* **30**, 1951–1963 (1994).
12. H. Ryoo, D. W. Kang, and J. W. Hahn, "Analysis of the effective reflectance of digital micromirror devices and process parameters for maskless photolithography," *Microelectron. Eng.* **88**, 235–239 (2011).
13. B.R. Brown and A.W. Lohmann "Computer-generated Binary Holograms," in *IBM Journal of Research and Development* **13**, 160–168 (1979).
14. Y.-X. Ren, M. Li, K. Huang, J.-G. Wu, H.-F. Gao, Z.-Q. Wang, and Y.-M. Li, "Experimental generation of Laguerre-Gaussian beam using digital micromirror device," *Applied optics* **49**, 1838–1844 (2010).
15. M. Mirhosseini, O. S. M. na Loaiza, C. Chen, B. Rodenburg, M. Malik, and R. W. Boyd, "Rapid generation of light beams carrying orbital angular momentum," *Opt. Express* **21**, 30196–30203 (2013).
16. V. Lerner, D. Shwa, Y. Drori, and N. Katz, "Shaping Laguerre–Gaussian laser modes with binary gratings using a digital micromirror device," *Optics letters* **37**, 4826–4828 (2012).
17. L. Gong, Y.-X. Ren, G.-S. Xue, Q.-C. Wang, J.-H. Zhou, M.-C. Zhong, Z.-Q. Wang, and Y.-M. Li, "Generation of nondiffracting Bessel beam using digital micromirror device," *Appl. Opt.* **52**, 4566–4575 (2013).
18. Q. Xu, Y. Wang, S. Siew, J. Lin, and Y. Zhang, "Generating self-accelerating Airy beams using a digital micromirror device," *Applied Physics B*, doi:10.1007/s00340-014-5813-2 (posted 7 May 2014, online).
19. R. Floyd and L. Steinberg, "An adaptive algorithm for spatial grey scale," in *Proc. Soc. Inf. Disp.* **17**, 75–77 (1976).